applied sciences

MDPI

Article

A Study on Mechanical Characteristics of Cement Composites Fabricated with Nano-Silica and Carbon Nanotube

Ali Raza [1], Manan Bhandari [1], Hyeong-Ki Kim [2], Hyeong-Min Son [3], Baofeng Huang [1] and Il-Woo Nam [4,*]

[1] College of Civil Engineering, Nanjing Tech University, Nanjing 211800, China; l20186110032@njtech.edu.cn (A.R.); L20186110030@njtech.edu.cn (M.B.); baofeng@njtech.edu.cn (B.H.)
[2] School of Architecture, Chosun University, Gwangju 61452, Korea; hyeongki@Chosun.ac.kr
[3] Department of Civil and Environmental Engineering, Korea Advanced Institute of Science and Technology, Daejeon 34141, Korea; nemilhm@kaist.ac.kr
[4] School of Spatial Environment System Engineering, Handong Global University, Gyeongbuk 37554, Korea
* Correspondence: namiru@handong.edu; Tel.: +82-54-260-1422

Abstract: In this study, cement composites were fabricated with various contents of added nano-silica (NS) and multi-walled carbon nanotubes (MWNTs). The compressive and flexural strengths of the resultant cement composites were examined. To explore the microstructures and MWNT distribution, electrical conductivity tests, and scanning electron microscopy were conducted. In addition, the strength results were analyzed based on thermal analysis and porosity evaluations. The electrical conductivity results indicated that MWNTs were satisfactorily distributed in the cement composites. In the mechanical strength tests, the composite with a 0.6% MWNT and 5% NS content and another with a 0.3% MWNT and 5% NS content yielded enhancements in the compressive and flexural strengths of 17.2% and 52% compared with the control samples, respectively. However, composites containing relatively large amounts of both NS and MWNTs showed degradation in the mechanical strength. The enhancement or degradation of the strength was supported by porosity evaluations and thermal analysis results. In particular, the degradation of the strength due to the incorporation of large amounts of both MWNTs and NS was explained by thermogravimetric analysis, which indicated a limited generation of calcium silicate hydrate (C-S-H) hydration products. The lower generation of C-S-H was likely due to the dense microstructure of MWNT/NS-incorporated cement hindering the reactions between calcium hydroxide and the NS.

Keywords: nano-silica; carbon nanotube; cement composites; mechanical strength; thermal analysis

check for updates

Citation: Raza, A.; Bhandari, M.; Kim, H.-K.; Son, H.-M.; Huang, B.; Nam, I.-W. A Study on Mechanical Characteristics of Cement Composites Fabricated with Nano-Silica and Carbon Nanotube. *Appl. Sci.* **2021**, *11*, 152. https://dx.doi.org/10.3390/app11010152

Received: 8 November 2020
Accepted: 21 December 2020
Published: 25 December 2020

Publisher's Note: MDPI stays neutral with regard to jurisdictional claims in published maps and institutional affiliations.

Copyright: © 2020 by the authors. Licensee MDPI, Basel, Switzerland. This article is an open access article distributed under the terms and conditions of the Creative Commons Attribution (CC BY) license (https://creativecommons.org/licenses/by/4.0/).

1. Introduction

Cementitious materials play a vital role in the construction industry [1,2]. Their complexity has not limited their range of applications. Concrete possesses many advantageous features, such as ease of production, low cost, high durability, versatility in molding, and energy efficiency [1–3]. In the past several decades, researchers have sought to enhance the physical properties of cementitious materials by utilizing nanomaterials [1,2,4–9]. A cement-based nanocomposites, which harness the advantages of nanomaterials, have attracted the attention of numerous researchers throughout the world [4–8].

Ultra-fine additives of cement-based materials include nano-silica (NS), carbon nanotubes (CNTs), nanoclay, and nano-Al_2O_3, and these additives have been the research subjects of numerous studies [5,9–12]. It was determined that NS introduces several beneficial characteristics when it is incorporated into cement, such as a reduction of the setting time and an increase in the calcium hydration products at early ages principally stemming from high pozzolanic reactivity with an exceptional surface area [13–15]. CNTs have remarkable characteristics due to their graphitic layers composed of carbon–carbon sp^2 bonding, which leads to a high stiffness and axial strength [16]. When they are embedded in cementitious materials, they contribute to enhancements in the mechanical

characteristics due to the pore-filling and bridging effects between the cement hydration products [9,17,18]. Nanoclay, also known as nano-metakaolin, is a silica-based product. It produces calcium silicate hydrate (C-S-H) gel by reacting with calcium hydroxide (CH) and enhances the early strength, resistance to alkali–silica reactions, and sulfate resistance when incorporated into concrete [9,17]. Nano-Al_2O_3 was also introduced to cementitious materials, resulting in enhancements in the mechanical characteristics, such as the modulus of elasticity, compressive strength, and split tensile strength [18,19]. These effects were attributed to high pozzolanic activity, which other inorganic nanomaterials exhibit [18].

Among those nanomaterials, NS and CNTs are most commonly chosen by researchers to impart outperforming physical characteristics to cement-based materials [10,19]. Both NS and CNTs can fill in the pores and decrease the pore diameters [11,14,20,21]. Furthermore, it is expected that NS may produce finer hydration products to enhance the anchorage of CNTs in the cement matrix. Meanwhile, it is often reported that CNTs are likely to agglomerate due to electrostatic attraction, and this results in deterioration in the physical characteristics of the resultant composites [1,22]. Multiple studies have demonstrated that silica materials help to distribute CNTs in cementitious materials [22–26]. Thus, it is expected that the presence of NS may improve the distribution uniformity of CNTs.

The representative studies in which NS and CNTs were utilized are summarized. Konsta–Gdoutos et al., 2010 examined the influence of the multi-walled carbon nanotube (MWNT) length on the flexural strengths of cementitious composites and concluded that the strength enhancement rate accomplished using long MWNTs (10–100 nm) with a content of 0.025–0.048 wt.% was comparable to that accomplished using short MWNTs (10–30 nm) with a content of 0.08 wt.% [27]. Parveen et al., 2015 utilized a novel dispersion agent, Pluronic F-127, to distribute single-walled carbon nanotubes (SWNTs) [28]. They also experimentally examined the optimal dosage of the agent and carried out flexural and compressive strength tests that showed enhancements of 7% and 19% after 28 d of curing, respectively, by incorporating 0.1% SWNT [28]. Naeem et al., 2017 demonstrated that mechanical and electro-mechanical properties were enhanced by incorporations of MWNT and silica fume [29]. In particular, mechanical properties of cement composites incorporating 0.6% MWNT and 10% silica fume showed increase of 36.07% and 18.11% in terms of compressive and flexural strengths, respectively [29]. Naqi et al., 2019 studied mechanical properties and autogenous shrinkage of MWNT-incorporated cement composites [30]. The authors demonstrated that 0.01% MWNT-incorporated cement composites brought 12.4% increase in compressive strength and 8.5% reduction in autogenous shrinkage [30].

Biricik and Sarier, 2014 compared the mechanical properties of NS, silica fume (SF), or fly ash (FA)-incorporated cement mortars and determined that the greatest enhancements in the compressive and flexural strengths of 84% and 32%, respectively, were achieved by incorporating 10% NS [13]. These improvements were higher than those of the control mortar after 28 days [13]. Snehal et al., 2020 investigated the early age setting, hydration, mechanical characteristics, and other properties of NS-incorporated cementitious composites [4]. In particular, the compressive strength was enhanced by 21% after 28 days compared to control mortar, and the mechanical characteristics were analyzed by thermogravimetric analysis (TGA), mineralogical characterization, and microstructure observations [4]. Hunashyal et al., 2014 achieved enhancements of the flexural and compressive strengths as high as 82.2% and 50.5% compared to plain cement paste, respectively, by incorporating 0.75% MWNTs and 0.5% NS simultaneously [10]. Lee et al., 2018 studied mechanical properties and durability of MWNT/NS-incorporated cement composites demonstrating enhanced corrosion resistance and increase of 12–76% in the compressive strength [31].

To date, various experimental studies have been conducted in which NS and/or CNTs were incorporated into the cementitious matrix. However, studies on the mechanical performances of cement composites fabricated with the simultaneous incorporation of NS and CNTs are scarce, and analyses on the enhancements of the mechanical characteristics by means of thermal analysis or porosity examinations have been inadequate.

In the present study, the mechanical characteristics of the cement composites fabricated with various contents of NS and CNTs were examined, and the measured mechanical characteristics were analyzed. MWNT/NS-incorporated cement composites were prepared by varying the MWNT content from 0% to 1.0% and the NS content from 0% to 5%. To understand the microstructure and CNT distribution, scanning electron microscopy (SEM) observations and electrical conductivity tests were performed. Moreover, TGA and porosity examinations were carried out to identify the factors affecting the enhancements of the mechanical characteristics.

2. Materials and Methods

In the present study, ordinary Portland cement was used as a primary binder. MWNTs, a product of Beijing DK nano technology Co., Ltd. in Beijing, China, were used, and their dimensions and physical properties are given in Table 1. NS, a product of SAT nano Technology Material Co., Ltd. in Dongguan, China, was used in a dry and fine powder form. The NS exhibited hydrophilic characteristics and had an SiO_2 content of 99.8%. The sizes and other details are provided in Table 2. The water used in the fabrication of the mixture was supplied from a tap. A polycarboxylic-acid-based super plasticizer (SP) was utilized for all sample preparations in an effort to control the fluidity of the fresh mixtures.

Table 1. Dimensions and physical properties of multi-walled carbon nanotubes (MWNTs).

Item	MWNT
Exterior diameter	<8 nm
Length	10–30 μm
Purity	98%
Ash	<0.5 wt.%
Specific surface area	>350 m^2/g
Electrical conductivity	>100 S/cm

Table 2. Dimensions and physical properties of nano-silica (NS).

Item	NS
Particle size	10–20 nm
pH	4–7
Specific surface area	170–220 m^2/g
SiO_2 content	99.8%

The mixture proportions and fabrication procedures of the cement composites were as follows. A total of 16 samples were prepared by adding different amounts of MWNT and NS. Four different NS contents, 0%, 1%, 3%, and 5% by weight of the cement were examined. In a similar fashion, four different MWNT contents, 0%, 0.3%, 0.6%, and 1% by weight of the cement were applied. The target flow of fresh mixture ranged from 127 to 166 mm, and all the mixtures were prepared in accordance with the target flow to enhance the distribution of nanomaterials [26,32]. Nam et al., 2015 and Kim et al., 2014 demonstrated that a fresh mixture prepared with a low fluidity led to enhancements of the MWNT distribution in the resultant cement composites [25,32]. Different amounts of the SP were used in the fresh mixtures, and the amount of SP varied based on the content of MWNTs used. The amounts of water and cement were fixed, and the SP content was varied in an effort to achieve the target flow. Details of the mixture proportions are given in Table 3.

Table 3. Constituent materials and mixture proportions of the MWNT/NS-incorporated cement composites.

Notation	MWNT	NS	W/B	SP/B	Flow Value (mm)
C0N0	0	0	0.26	0.003	195
C0N1	-	1	-	-	166
C0N3	-	3	-	-	141
C0N5	-	5	-	-	133
C0.3N0	0.3	0	0.26	0.0067	163
C0.3N1	-	1	-	-	131
C0.3N3	-	3	-	-	127
C0.3N5	-	5	-	-	126
C0.6N0	0.6	0	0.26	0.013	150
C0.6N1	-	1	-	-	139
C0.6N3	-	3	-	-	130
C0.6N5	-	5	-	-	135
C1.0N0	1.0	0	0.26	0.022	131
C1.0N1	-	1	-	-	127
C1.0N3	-	3	-	-	127
C1.0N5	-	5	-	-	127

To ensure the integrity of the composite samples, the following fabrication procedures were carefully followed. Cement, NS, and MWNTs were weighed based on the specified proportions, and the mixture was poured into the bowl of an automatic mixer. Dry mixing was conducted for 3–4 min for preliminary mixing. After the pre-mixing, water and SP were added to the dry mixture and mixed again for another 2 min. A flow test was carried out to examine the fluidity, and the fresh mixture was decanted into molds with dimensions of 40 mm by 40 mm by 160 mm if the flow value was in the target flow range. The fresh mixtures in the molds were placed on a table-type vibrator and compacted for 60 s. The mixtures were subsequently cured in a storage cabinet under an ambient temperature of 18–20 °C for 28 days. Figure 1 shows images captured in each step of the fabrication procedure.

Figure 1. Schematic illustrating the fabrication procedures of the multi-walled carbon nanotubes/nano-silica (MWNT/NS)-incorporated cement composites.

The testing methods are briefly described as follows. A three-point flexural test was conducted in compliance with American Society for Testing and Materials (ASTM) C 78 after 28 days of sample curing. The fabricated prismatic composite samples were subjected to flexural loading applied with a displacement-control loading system. The

loading speed was 0.002 mm/s. Five composite samples for each sample type were tested, and the determined strength values were averaged. The compressive strengths of the composites were measured after 28 days of curing according to the ASTM C 109. Four composite samples were tested for each sample type, and the determined strength values were averaged.

To assess the electrical conductivities of the composites, a two-probe method was employed. Before evaluating the conductivity, silver paste was first applied to both sides of the composite sample, and then copper foil was attached to the silver-paste-covered surfaces. The silver paste was used in an effort to decrease the contact resistance produced between the copper foil and the composite. The newly added copper foils were connected to two probes of a digital multimeter (Keysight, DMM34461A; Keysight Technologies, Santa Rosa, CA, USA), and the electrical resistance was assessed. Electrical resistance measurements were conducted for two samples of each composite type, and the determined values were averaged. The electrical resistance was converted to an electrical conductivity with consideration of the composite sample dimension. An equation that converts electrical resistance measured by the two-probe method to electrical conductivity was provided as follows [23,33].

$$\sigma = \frac{1}{\rho} = \frac{L}{R \times A} \quad (1)$$

where σ and ρ denote electrical conductivity and resistivity, respectively. R indicates electrical resistance measured from the samples. L and A denote distance between the electrodes and cross sectional area of sample that is contacted to the electrode, respectively [23,33]. Details of the electrical conductivity assessment can be found in the publications of Kim et al., 2018 and Wang et al., 2020 [23,33].

Porosity of the cement composite, which is defined as a ratio of the volume of water and air to total volume of the composite, was measured in accordance with the ASTM C 642 [34]. In porosity measurement, the prismatic parallelepiped cement composites with dimension of 40 mm by 40 mm by 160 mm were used and a following formula having parameters of A, B, and C was used [34].

$$\text{Porosity (vol.\%)} = \frac{C - A}{C - B} \times 100 \quad (2)$$

where A indicates mass of the cement samples dried at 110 °C for 24 h [34]. B indicates apparent mass of the samples suspended in water after they were immersed and boiled [34]. C denotes mass of the surface-dried samples after they were immersed and boiled [34]. Details of test procedure can be found in the publication of Nam et al., 2016 [34].

To observe the microstructures of the composites, fractured surface images were obtained by means of SEM (JEOL Ltd. in Tokyo, Japan, Model: JSM-6300). The composite samples for SEM observations were fabricated separately from the composite samples fabricated for the mechanical strength tests. The mixture proportions and fabrication procedure were identical to those mentioned earlier, but product models of the MWNTs and NS were not identical. In the sample preparation for the SEM observations, MWNTs, a product of Hyosung Inc. in Seoul, South Korea (Product model: M1111), were used. The diameter and purity of the MWNTs were 12.29 ± 2.18 nm and 96.2%, respectively, which were comparable to those of the MWNTs used in the samples of the mechanical tests. In addition, NS, a product of OCI chemicals Inc. (Seoul, South Korea) was used, and the specific surface areas (approximately 200 m^2/g) and diameters (10–30 nm) of the NS particles were comparable to those of the NS used in the samples of the mechanical tests. After 28 days of sample curing, the composite samples were crushed and mounted on the sample holder of a scanning electron microscope to observe the fractured surfaces.

Mass change of the MWNT/NS-incorporated cement composites was examined using thermogravimetric analyzer (Mettler-toledo Inc. in Columbus, OH, USA, Model: TGA/DSC1/1600 LF) while the sample is subjected to gradual transition of the temperature from 31 °C to 998 °C.

3. Results

3.1. Electrical Conductivity

Figure 2 shows the electrical conductivities of MWNT/NS-incorporated cement composites as functions of the MWNT content on a logarithmic scale. In all the sample groups, which are denoted as NS0, NS1, NS3, and NS5, an exponential increase in the electrical conductivity occurred as the MWNT increased. This exponential increase, which is often called an "S-curve," can be found in the electrical conductivity results of the conductive-filler-incorporated cement composites reported in the literature, and this was due to the conductive fillers being evenly distributed in the cement matrix [26,34,35]. This principle can be applied to the present work in the same manner. The exponential increase in the electrical conductivity represents an even distribution of MWNTs in the cement matrix. In addition to the electrical conductivity results, color examination by the naked eye further suggested the even distribution of MWNTs. The greater the MWNT content, the darker the composite samples examined became.

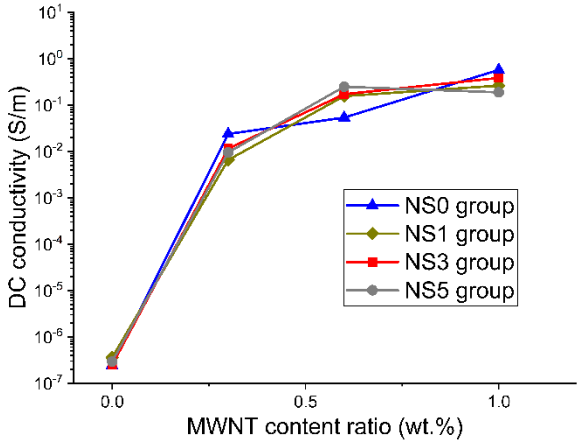

Figure 2. Electrical conductivity (logarithmic scale) variations with the MWNT content.

In the relationship of the MWNT content and electrical conductivity, the percolation threshold, which is the particular range of MWNT contents where a prominent increase in the conductivity occurred, was in the range of 0–0.3%. This percolation threshold range can be found in previous studies in which the electrical characteristics of the carbon-nanotube-added cement composites were explored [26,34]. The percolation threshold range and electrical conductivity levels in each group shown in Figure 2 showed marginal differences. Accordingly, it was inferred that NS, which was an electrically insulating material, did not produce adverse effects on the conductive MWNT networks.

The effect of the silica fume incorporation on the electrical characteristics of MWNT-added cement composites has been explored in previous studies. Nam et al., 2012 and Kim et al., 2014 concluded that silica fume incorporation with an appropriate content yielded improvements in the distribution of MWNTs due to breaking of the electrostatic attraction of the MWNTs by means of silica fume particles, and this, in turn, led to an enhancement of the electrical conductivities of the composites [24,25]. Silica fume with an average diameter greater than 5 μm was used in these previous studies [24,25]. However, in the present study, the diameters of the NS particles were 10–20 nm, which was close to the diameters of the MWNTs. This considerable difference in the diameters of the siliceous materials may have resulted in different outcomes, which means siliceous materials whose diameters were as small as the diameters of MWNTs were not likely to improve conductive MWNT networks.

3.2. Mechanical Strength

In Figure 3a, the samples were grouped as MWNT0, MWNT0.3, MWNT0.6, and MWNT1.0, and the compressive strength results are presented as a function of NS content. In the MWNT0, MWNT0.3, and MWNT0.6 groups, the compressive strengths tended to increase with the addition of NS, and the largest increment reached 8.6%, 9.5%, and 29.2% compared to the strength of the composite without NS, respectively. However, the increasing tendency was not pronounced for the MWNT1.0 group. In the MWNT1.0 group, enhancements of the compressive strength were achieved by the incorporation of 1% and 3% NS, but the compressive strength dropped due to the incorporation of 5% NS, which is considered to be a relatively large NS content.

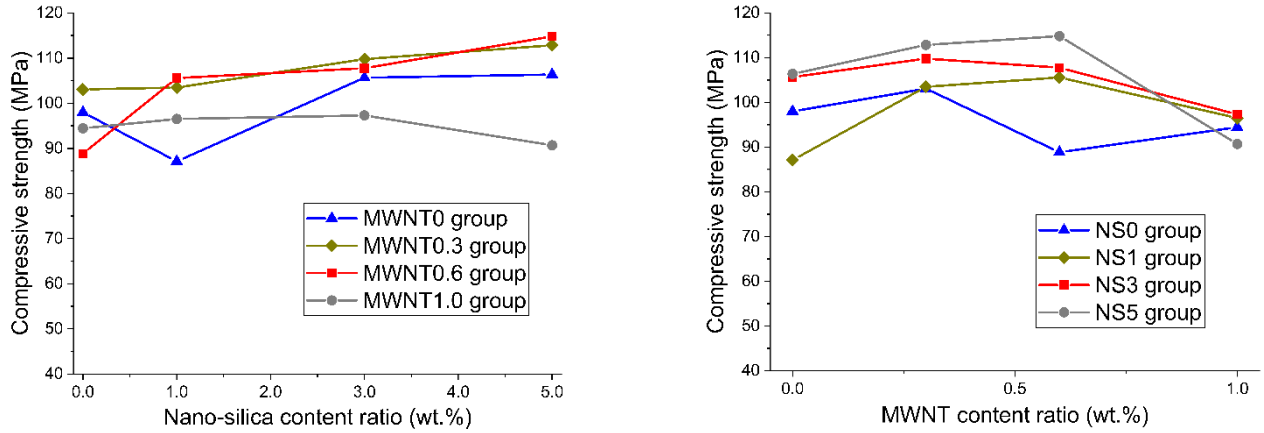

Figure 3. Compressive strength results of the MWNT/NS-incorporated cement composites after 28 days of curing: (**a**) NS content varied and (**b**) MWNT content varied.

Figure 3b shows that compressive strengths of the NS0, NS1, NS3, and NS5 groups varied as the content of MWNTs increased. In all the groups, the increase in the compressive strength was significant when the MWNT contents were 0.3% or 0.6% compared to the strength of the composite without MWNTs. The largest increases were 5.2%, 21.2%, 3.9%, and 8.0% in the NS0, NS1, NS3, and NS5 groups, respectively.

In the view of the compressive strength results of all the composites, it is noteworthy that enhancement of the strength was the largest in the composite with 0.6% MWNTs and 5% NS (corresponding to a strength of 114.8 MPa), which was 17.2% greater than the strength of the control with no MWNTs and NS. The best enhancement rate and strength level were not achieved by the incorporation of a single nanomaterial, that is, either MWNT or NS alone. This signified a synergistic effect of the MWNTs and NS on the compressive strengths of the composites. However, in the composite groups having relatively large amounts of NS, such as the NS3 and NS5 groups, the compressive strength decreased due to the incorporation of 1% MWNTs, which is considered to be a relatively large MWNT content. Naqi et al., 2019 demonstrated that compressive strength increased when appropriate amount of MWNT was incorporated in the cement composites, and discussed that this outcome was accomplished due to that distributed MWNT played a role of additional nucleation site to form C-S-H [30]. Accordingly, it can be said that appropriate amount of MWNT can provide additional nucleation site for C-S-H formation, and addition of NS promoted C-S-H generation, which ultimately lead to synergistic effects in the compressive strength.

Figure 4a shows the flexural strength results of the MWNT0, MWNT0.3, MWNT0.6, and MWNT1.0 groups as a function of the NS content. Similar to the compressive results shown in Figure 3a, enhancements of the flexural strength with the addition of NS were evident in the MWNT0, MWNT0.3, and MWNT0.6 groups, and the greatest increases

reached 30.6%, 9.9%, and 14.3%, respectively. In contrast, a decrease in the flexural strength was evident in the MWNT1.0 group, of which the MWNT content was relatively large, and this outcome was similar to the compressive strength results of the MWNT1.0 group shown in Figure 3a.

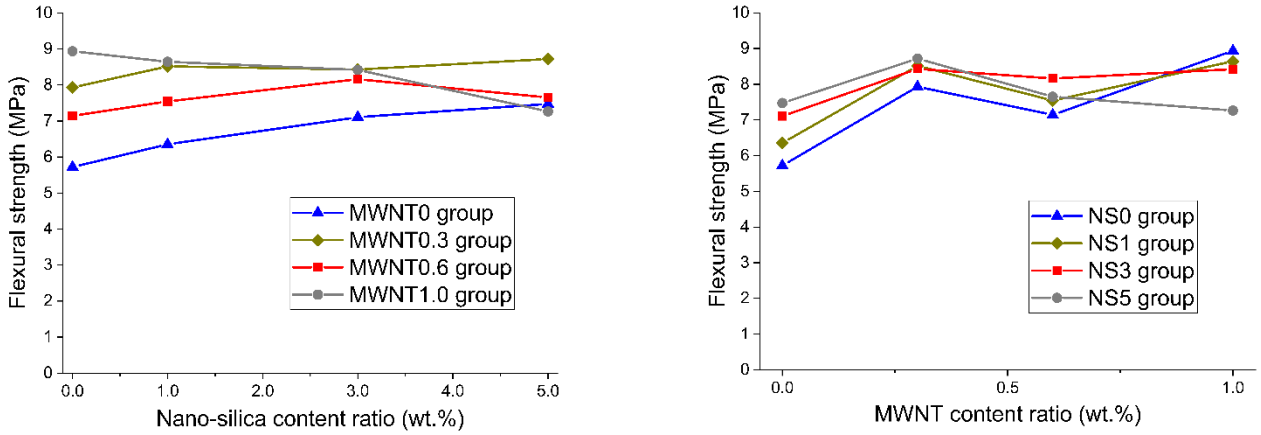

Figure 4. Flexural strength results of the MWNT/NS-incorporated cement composites after 28 days of curing: (**a**) NS content varied and (**b**) MWNT content varied.

Figure 4b shows that the flexural strengths of the NS0, NS1, NS3, and NS5 groups changed as the MWNT content ratio varied. In all the groups, the compressive strength increased due to the incorporation of 0.3% or 1.0% MWNTs compared to the strength of the composite without MWNT. The largest increases in the NS0, NS1, NS3, and NS5 groups were 56.2%, 36.1%, 18.5%, and 16.7%, respectively. However, in the composite groups fabricated with relatively large amounts of NS, such as the NS3 and NS5 groups, it was found that the incorporation of 1% MWNTs led to a marginal enhancement or deterioration of the strength.

In the view of the flexural strength results of all the composites, the composite type with 0.3% MWNT and 5% NS (corresponding to a strength of 8.7 MPa) achieved the largest enhancement of 52% compared to the control with no MWNTs and NS. This signified that a prominent enhancement in the flexural strength could be accomplished by the simultaneous utilization of MWNTs and NS.

The enhancements of the compressive and flexural strengths were achieved by incorporation of the appropriate amounts of MWNTs and NS, but additions of MWNTs and NS were detrimental to the mechanical strength of the composites when both nanomaterials were excessively utilized.

3.3. Porosity

Figure 5a shows the porosity of the MWNT/NS-incorporated cement composites as a function of the NS content, and the composites were grouped as MWNT0, MWNT0.3, MWNT0.6, and MWNT1.0. The porosity tended to decrease with the addition of NS in the MWNT0, MWNT0.3, and MWNT0.6 groups. It is noteworthy that the enhancements of compressive and flexural strengths in the MWNT0, MWNT0.3, and MWNT0.6 groups shown in Figures 3a and 4a were closely related to the decrease in the porosity. Meanwhile, the decrease in the porosity for the MWNT1.0 group was not pronounced. This was likely because the densification of the microstructure developed by NS addition was minor, particularly for the MWNT1.0 group.

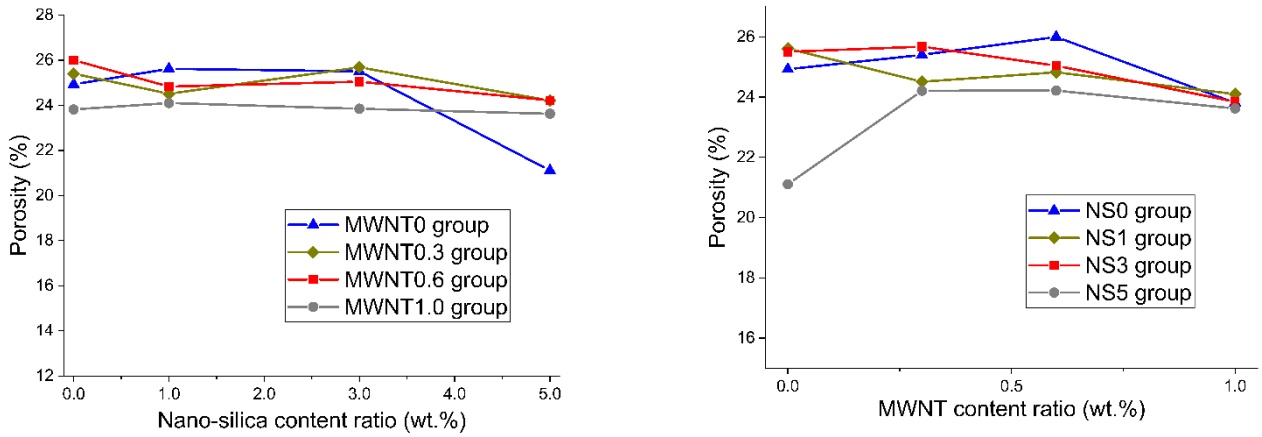

Figure 5. The porosity results of the MWNT/NS-incorporated cement composites: (**a**) NS content varied and (**b**) MWNT content varied.

Figure 5b shows the porosity results as a function of the MWNT content. The porosity tended to decrease with the addition of MWNTs in the NS0, NS1, and NS3 groups. In contrast, the porosity tended to increase with the MWNT content in the NS5 group, which was prepared with a relatively large amount of NS. This outcome was closely related to the compressive and flexural strength results of the NS5 group shown in Figures 3b and 4b, respectively, which represented a decrease in strength due to the addition of 1% MWNT.

3.4. Scanning Electron Microscopy (SEM)

Figure 6a–p show the morphologies of the fractured surfaces of the MWNT/NS-incorporated cement composites observed by SEM. To provide the further morphological data, supplementary SEM images are presented in Figure S1. C-S-H, which is a flat and broad hydration product, was more visible when the NS content was greater [13,36]. In most of fractured surfaces, NS particles were not found, and this is likely due to that NS already underwent pozzolanic reactions. In the MWNT-incorporated composite types, most of MWNTs were not agglomerated and were distributed in a separated form. It was observed that diameter of MWNT was approximately 10 nm and length was several micrometers. In addition, it was found that the separated MWNTs were anchored in hydration products (e.g., Figure 6f–p) and MWNTs played the role of bridge (e.g., Figure 6f), which contributed to enhancements in mechanical strength. On the other hand, agglomerated MWNTs were detected in the C1.0N5 composite, which was prepared with relatively large amounts of MWNTs and NS. Unlike individual CNT strands, which led to bridging and packing effects in the cement hydrate or interface, the agglomerated CNTs did not yield these positive effects, but rather they acted similarly to pores in the microstructure of the cement composites [25,37].

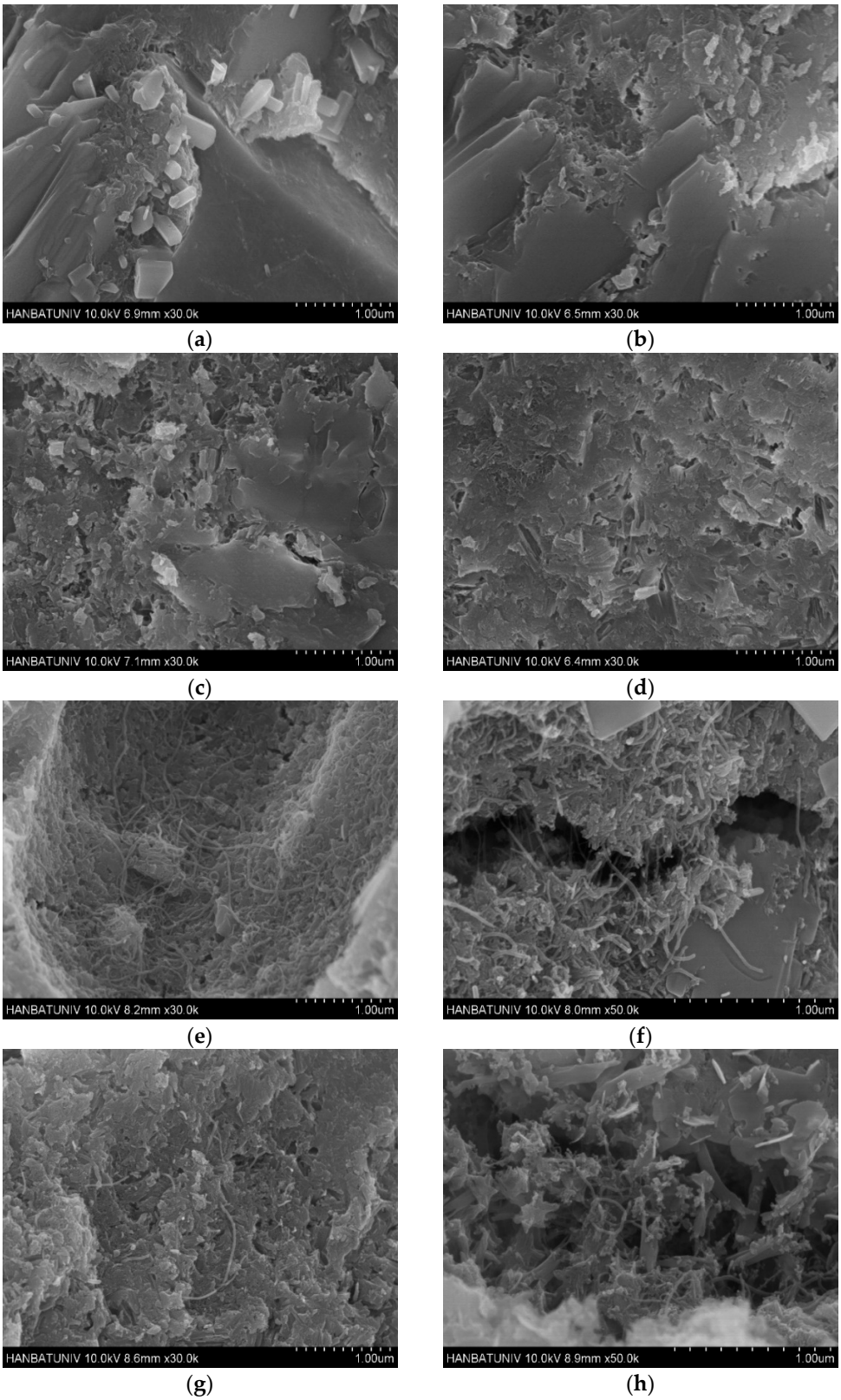

Figure 6. *Cont.*

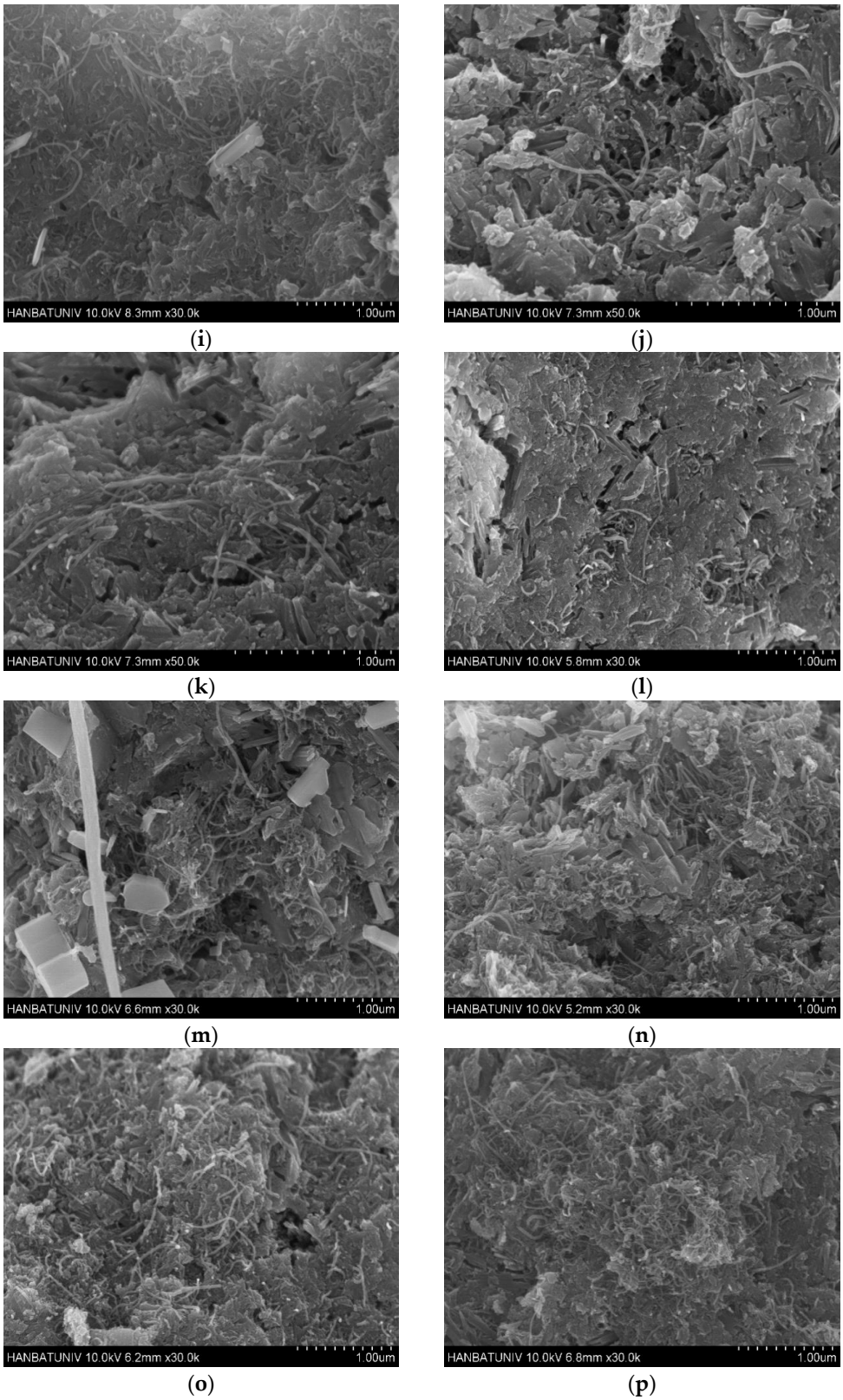

Figure 6. Scanning electron microscopy (SEM) images obtained from the fractured surfaces of each composite type, (**a**) C0N0, (**b**) C0N1, (**c**) C0N3, (**d**) C0N5, (**e**) C0.3N0, (**f**) C0.3N1, (**g**) C0.3N3, (**h**) C0.3N5, (**i**) C0.6N0, (**j**) C0.6N1, (**k**) C0.6N3, (**l**) C0.6N5, (**m**) C1.0N0, (**n**) C1.0N1, (**o**) C1.0N3, (**p**) C1.0N5.

3.5. Thermogravimetric Analysis (TGA)

Figure 7a,b presents the TGA results obtained by recording the mass loss when the cement composites in the MWNT0.3 and MWNT1.0 groups were subjected to progressive heating from 31 °C to 998 °C. Mass losses primarily occurred within two temperature ranges. The first range was between 31 °C and 200 °C, where water molecules dehydrated from the calcium silicate hydrate gel [4,13,36,38]. Therefore, the mass loss in the first range signified the amount of C-S-H produced by cement hydration in the composite [4,13,36,38]. The second range was between 325 °C and 550 °C, where calcium hydroxide (also known as portlandite) decomposed, and the mass loss in this range represented the amount of CH produced as a result of cement hydration [4,13,36,38]. Since CH can undergo a pozzolanic reaction with NS, and the reaction results in the formation of additional C-S-H, the reduction of the CH mass loss shown in the MWNT0.3 group and MWNT1.0 group of Table 4 signified an increased amount of C-S-H [4,13,36,38].

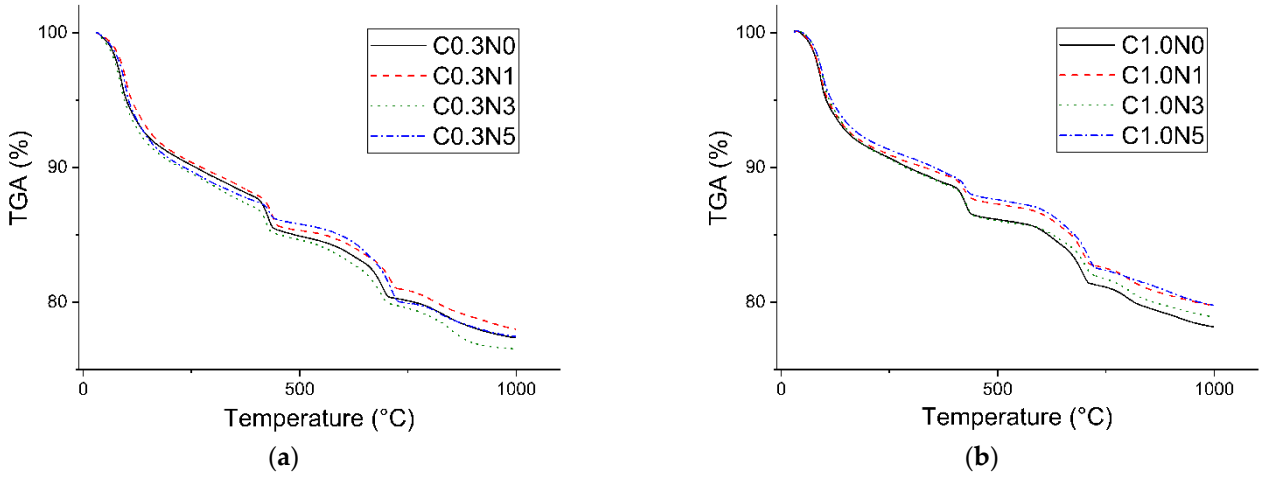

Figure 7. The thermogravimetric analysis (TGA) assessed for (**a**) MWNT0.3 group and (**b**) MWNT1.0 group.

Table 4. Mass loss results computed from two different ranges of TGA.

-	Temp.	C0.3N0	C0.3N1	C0.3N3	C0.3N5	C1.0N0	C1.0N1	C1.0N3	C1.0N5
1st range	31–200 °C	8.9	8.7	9.6	9.4	8.5	8.4	8.6	8
2nd range	325–550 °C	4.4	4.2	4.1	3	3.7	3.1	3.7	3.1

The mass losses computed from each composite in the first and second temperature ranges are presented in Table 4 and Figure 8. The mass loss in the first range increased with the increase in the NS content in the MWNT0.3 group, which indicated an increase in the amount of C-S-H due to the addition of NS. Meanwhile, a trend of the mass loss in the first range in the MWNT1.0 group was dissimilar to that obtained in the MWNT0.3 group. In the MWNT1.0 group, an increase in the mass loss with the increase in the NS content did not occur, which indicated that an increase in the C-S-H generation due to NS addition was not noticeable. When the amount of the incorporated-MWNT was relatively large, the structure of the cement composite was dense, and this hindered the contact between the CH and NS. This hindrance prevented the formation of additional C-S-H. This may have negatively affected the reinforcement effect of the NS on the mechanical properties due to the sluggish generation of C-S-H, which transports mechanical forces. This agrees with marginal changes of the porosity in the MWNT1.0 group and small changes or deterioration in the compressive and flexural strengths of the MWNT1.0 group shown in Figures 3a, 4a, and 5a, respectively.

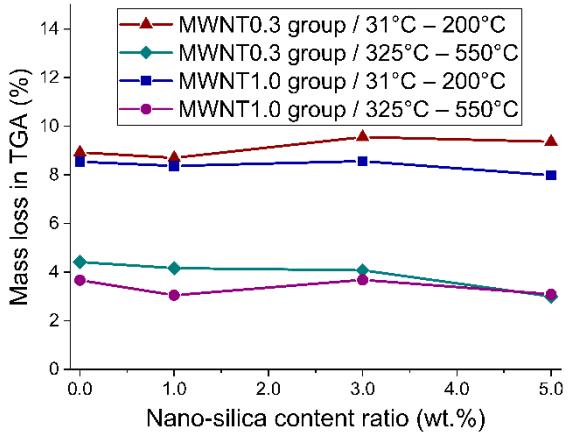

Figure 8. Mass losses computed at two different ranges during TGA.

In the second range, the decomposed portion in the MWNT0.3 and MWNT1.0 groups tended to decrease with the increase in the NS, which means that more CH underwent a pozzolanic reaction with NS [4,13,36,38]. In addition, mass loss in the MWNT1.0 group was smaller than that in the MWNT0.3 group. In particular, the mass loss of C0.3N0 dropped by 31.8% as the NS content increased to 5%, whereas the mass loss of C1.0N0 only dropped by 16.7% as the NS content increased to 5%. This indicated that the cement composites of the MWNT1.0 group utilized a limited amount of CH, relatively less than that utilized in the MWNT0.3 group, though the amount of incorporated NS increased. This finding supports the aforementioned discussion of the dense microstructure due to incorporation of 1% MWNT, which hindered the pozzolanic reaction between CH and NS.

4. Conclusions

In this study, the cement composites were prepared by adding various contents of MWNTs and NS. The microstructure and MWNT distribution were examined using SEM images and electrical conductivity tests. The compressive and flexural strengths of the composites were tested, and they were analyzed using thermal analysis and porosity evaluations. The experimental findings are summarized as follows.

The exponential increase in the electrical conductivity with the increase in the MWNT content indicated that the MWNTs were satisfactorily distributed in the cement composites. The percolation threshold of all the composite types was shown in the range between MWNT 0% and 0.3%. The similar level of the percolation threshold with regardless of the composite type represents that contribution of NS addition to the electrical characteristics of the composites was insignificant. However, it is noteworthy that NS, which is an insulating material, did not have an adverse effect on the conductive MWNT networks.

The composite type with 0.6% MWNTs and 5% NS and the composite type with 0.3% MWNTs and 5% NS exhibited enhancements of the compressive and flexural strengths of 17.2% and 52% compared to the control samples, respectively. In particular, the 17.2% enhancement rate of the compressive strength was only achieved by the simultaneous incorporation of MWNT and NS. This signified a synergistic effect of the MWNTs and NS on the compressive strengths. It was discussed that addition of NS promoted C-S-H generation and the distributed MWNT played a role of additional nucleation site to form C-S-H. However, composites with relatively large amounts of NS and MWNTs, e.g., the C1.0N5 composite, showed degradation in the mechanical strength.

The porosity results agreed with the mechanical strength results. The porosity tended to decrease as the NS or MWNT content increased in the composites, but this was not applicable to the composite types that included relatively large amounts of NS and MWNTs, e.g., C1.0N5. This was likely because the densification of the microstructure developed by NS addition was minor.

In the microstructural observations, it was apparent that MWNTs were distributed and embedded in the cement hydration products. However, agglomerated MWNTs were found in the C1.0N5 composite, and in the best endeavors of the authors, those were not found in other composite types. Unlike individual CNT strands, which led to a bridging and packing effects in the cement hydrate or interface, the agglomerated CNTs did not yield these positive effects, but rather they acted similarly to pores in the microstructure of the cement composites.

The thermal analysis agreed with the porosity and mechanical strength results. In the composite including a relatively large amount of MWNTs and NS, C-S-H generation was reduced. This agrees with marginal changes of the porosity in the MWNT1.0 group and small changes or deterioration in the compressive and flexural strengths of the MWNT1.0 group.

Additional C-S-H generation due to the reaction between NS and CH was limited due to the dense microstructure of the MWNT/NS-incorporated cement, although the incorporation ratio of NS increased. This finding endorses insignificant change of the porosity in the MWNT1.0 group and minor changes or decrease in the compressive/flexural strengths of the MWNT1.0 group which possesses relatively dense microstructure.

Supplementary Materials: The following are available online at https://www.mdpi.com/2076-3417/11/1/152/s1, Figure S1: Additional SEM images obtained from the fractured surfaces of each composite type.

Author Contributions: Conceptualization, I.-W.N. and H.-K.K.; methodology, I.-W.N. and H.-K.K.; formal analysis, A.R., I.-W.N., and H.-K.K.; investigation, A.R., M.B., and H.-M.S.; data curation, A.R., M.B., and H.-M.S.; writing—original draft preparation, A.R. and I.-W.N.; writing—review and editing, I.-W.N., B.H., and H.-K.K.; visualization, A.R. and I.-W.N.; supervision, I.-W.N. and H.-K.K.; project administration, B.H. and I.-W.N.; funding acquisition, I.-W.N. All authors have read and agreed to the published version of the manuscript.

Funding: This study was sponsored by the National Natural Science Foundation of China (NSFC) (51950410578).

Institutional Review Board Statement: Not applicable.

Informed Consent Statement: Not applicable.

Data Availability Statement: The data presented in this study are available on request from the corresponding author. The data are not publicly available to prevent indiscreet replications.

Acknowledgments: Authors acknowledge the collaborative efforts made by J.C. Wang and X.D. Wang when the experiments and analysis were carried out.

Conflicts of Interest: The authors declare no conflict of interest. The funders had no role in the design of the study; in the collection, analyses, or interpretation of data; in the writing of the manuscript, or in the decision to publish the results.

References

1. Sanchez, F.; Sobolev, K. Nanotechnology in concrete—A review. *Constr. Build. Mater.* **2010**, *24*, 2060–2071. [CrossRef]
2. Chuah, S.; Pan, Z.; Sanjayan, J.G.; Wang, C.M.; Duan, W.H. Nano reinforced cement and concrete composites and new perspective from graphene oxide. *Constr. Build. Mater.* **2014**, *73*, 113–124. [CrossRef]
3. Zhang, G.Z.; Cho, H.K.; Wang, X.Y. Effect of nano-silica on the autogenous shrinkage, strength, and hydration heat of ultra-high strength concrete. *Appl. Sci.* **2020**, *10*, 5202. [CrossRef]
4. Snehal, K.; Das, B.B.; Akanksha, M. Early age, hydration, mechanical and microstructure properties of nano-silica blended cementitious composites. *Constr. Build. Mater.* **2020**, *233*, 117212. [CrossRef]
5. Gopinath, S.; Mouli, P.C.; Murthy, A.R.; Iyer, N.R.; Maheswaran, S. Effect of nano silica on mechanical properties and durability of normal strength concrete. *Arch. Civ. Eng.* **2012**, *58*, 433–444. [CrossRef]
6. Al Ghabban, A.; Al Zubaidi, A.B.; Jafar, M.; Fakhri, Z. Effect of Nano SiO_2 and Nano $CaCO_3$ on the Mechanical Properties, Durability and flowability of Concrete. *IOP Conf. Ser. Mater. Sci. Eng.* **2018**, *454*, 12016. [CrossRef]
7. Khaloo, A.R.; Vayghan, A.G.; Bolhasani, M. Mechanical and microstructural properties of cement paste incorporating nano silica particles with various specific surface areas. *Key Eng. Mater.* **2011**, *478*, 19–24. [CrossRef]

8. Nasibulina, L.I.; Anoshkin, I.V.; Nasibulin, A.G.; Cwirzen, A.; Penttala, V.; Kauppinen, E.I. Effect of carbon nanotube aqueous dispersion quality on mechanical properties of cement composite. *J. Nanomater.* **2012**, 169262. [CrossRef]
9. Morsy, M.S.; Alsayed, S.H.; Aqel, M. Hybrid effect of carbon nanotube and nano-clay on physico-mechanical properties of cement mortar. *Constr. Build. Mater.* **2011**, *25*, 145–149. [CrossRef]
10. Hunashyal, A. Experimental Investigation on the Effect of Multiwalled Carbon Nanotubes and Nano-SiO_2 Addition on Mechanical Properties of Hardened Cement Paste. *Adv. Mater.* **2014**, *3*, 45. [CrossRef]
11. Stefanidou, M.; Papayianni, I. Influence of nano-SiO 2 on the Portland cement pastes. *Compos. Part B Eng.* **2012**, *43*, 2706–2710. [CrossRef]
12. Rai, S.; Tiwari, S. Nano Silica in Cement Hydration. *Mater. Today Proc.* **2018**, *5*, 9196–9202. [CrossRef]
13. Biricik, H.; Sarier, N. Comparative Study of the Characteristics of Nano Silica-, Silica Fume- and Fly Ash-Incorporated Cement Mortars. *Mater. Res.* **2014**, *17*, 570–582. [CrossRef]
14. Kim, T.; Hong, S.; Seo, K.Y.; Kang, C. Characteristics of Ordinary Portland cement using the New Colloidal Nano-Silica mixing method. *Appl. Sci.* **2019**, *9*, 4358. [CrossRef]
15. Ltifi, M.; Guefrech, A.; Mounanga, P.; Khelidj, A. Experimental study of the effect of addition of nano-silica on the behaviour of cement mortars. *Procedia Eng.* **2011**, *10*, 900–905. [CrossRef]
16. Siddique, R.; Mehta, A. Effect of carbon nanotubes on properties of cement mortars. *Constr. Build. Mater.* **2014**, *50*, 116–129. [CrossRef]
17. Kumar, R.; Mohd Yaseen, A.Y.B.; Shafiq, N.; Jalal, A. Influence of metakaolin, fly ash and nano silica on mechanical and durability properties of concrete. *Key Eng. Mater.* **2017**, *744*, 8–14. [CrossRef]
18. Mohseni, E.; Miyandehi, B.M.; Yang, J.; Yazdi, M.A. Single and combined effects of nano-SiO_2, nano-Al_2O_3 and nano-TiO_2 on the mechanical, rheological and durability properties of self-compacting mortar containing fly ash. *Constr. Build. Mater.* **2015**, *84*, 331–340. [CrossRef]
19. Singh, L.P.; Karade, S.R.; Bhattacharyya, S.K.; Yousuf, M.M.; Ahalawat, S. Beneficial role of nanosilica in cement based materials—A review. *Constr. Build. Mater.* **2013**, *47*, 1069–1077. [CrossRef]
20. Xu, S.; Liu, J.; Li, Q. Mechanical properties and microstructure of multi-walled carbon nanotube-reinforced cement paste. *Constr. Build. Mater.* **2015**, *76*, 16–23. [CrossRef]
21. Ortega, J.M.; García-Vera, V.E.; Solak, A.M.; Tenza-Abril, A.J. Pore structure degradation of different cement mortars exposed to sulphuric acid. *Appl. Sci.* **2019**, *9*, 5297. [CrossRef]
22. Kim, G.M.; Nam, I.W.; Yang, B.; Yoon, H.N.; Lee, H.K.; Park, S. Carbon nanotube (CNT) incorporated cementitious composites for functional construction materials: The state of the art. *Compos. Struct.* **2019**, *227*, 111244. [CrossRef]
23. Kim, G.M.; Nam, I.W.; Yoon, H.N.; Lee, H.K. Effect of superplasticizer type and siliceous materials on the dispersion of carbon nanotube in cementitious composites. *Compos. Struct.* **2018**, *185*, 264–272. [CrossRef]
24. Nam, I.W.; Kim, H.K.; Lee, H.K. Influence of silica fume additions on electromagnetic interference shielding effectiveness of multi-walled carbon nanotube/cement composites. *Constr. Build. Mater.* **2012**, *30*, 480–487. [CrossRef]
25. Kim, H.K.; Nam, I.W.; Lee, H.K. Enhanced effect of carbon nanotube on mechanical and electrical properties of cement composites by incorporation of silica fume. *Compos. Struct.* **2014**, *107*, 60–69. [CrossRef]
26. Nam, I.W.; Choi, J.H.; Kim, C.G.; Lee, H.K. Fabrication and design of electromagnetic wave absorber composed of carbon nanotube-incorporated cement composites. *Compos. Struct.* **2018**. [CrossRef]
27. Konsta-Gdoutos, M.S.; Metaxa, Z.S.; Shah, S.P. Highly dispersed carbon nanotube reinforced cement based materials. *Cem. Concr. Res.* **2010**, *40*, 1052–1059. [CrossRef]
28. Parveen, S.; Rana, S.; Fangueiro, R.; Paiva, M.C. Microstructure and mechanical properties of carbon nanotube reinforced cementitious composites developed using a novel dispersion technique. *Cem. Concr. Res.* **2015**, *73*, 215–227. [CrossRef]
29. Naeem, F.; Lee, H.K.; Kim, H.K.; Nam, I.W. Flexural stress and crack sensing capabilities of MWNT/cement composites. *Compos. Struct.* **2017**, *175*. [CrossRef]
30. Naqi, A.; Abbas, N.; Zahra, N.; Hussain, A.; Shabbir, S.Q. Effect of multi-walled carbon nanotubes (MWCNTs) on the strength development of cementitious materials. *J. Mater. Res. Technol.* **2019**, *8*, 1203–1211. [CrossRef]
31. Lee, H.S.; Balasubramanian, B.; Gopalakrishna, G.V.T.; Kwon, S.J.; Karthick, S.P.; Saraswathy, V. Durability performance of CNT and nanosilica admixed cement mortar. *Constr. Build. Mater.* **2018**, *159*, 463–472. [CrossRef]
32. Nam, I.W.; Lee, H.K. Image Analysis and DC Conductivity Measurement for the Evaluation of Carbon Nanotube Distribution in Cement Matrix. *Int. J. Concr. Struct. Mater.* **2015**, *9*. [CrossRef]
33. Wang, X.D.; Wang, J.C.; Biswas, S.; Kim, H.; Nam, I.W. Mechanical, Electrical, and Piezoresistive Sensing Characteristics of Epoxy-Based Composites Incorporating Hybridized Networks of Carbon Nanotubes, Graphene, Carbon Nanofibers, or Graphite Nanoplatelets. *Sensors* **2020**, *20*, 2094. [CrossRef] [PubMed]
34. Nam, I.W.; Souri, H.; Lee, H.K. Percolation threshold and piezoresistive response of multi-wall carbon nanotube/cement composites. *Smart Struct. Syst.* **2016**, *18*. [CrossRef]
35. Xie, P.; Gu, P.; Beaudoin, J.J. Electrical percolation phenomena in cement composites containing conductive fibres. *J. Mater. Sci.* **1996**, *31*, 4093–4097. [CrossRef]
36. Zhang, L.; Ma, N.; Wang, Y.; Han, B.; Cui, X.; Yu, X.; Ou, J. Study on the reinforcing mechanisms of nano silica to cement-based materials with theoretical calculation and experimental evidence. *J. Compos. Mater.* **2016**, *50*, 4135–4146. [CrossRef]

37. Li, W.; Ji, W.; Isfahani, F.T.; Wang, Y.; Li, G.; Liu, Y.; Xing, F. Nano-silica sol-gel and carbon nanotube coupling effect on the performance of cement-based materials. *Nanomaterials* **2017**, *7*, 185. [CrossRef]
38. Hou, P.; Kawashima, S.; Kong, D.; Corr, D.J.; Qian, J.; Shah, S.P. Modification effects of colloidal nanoSiO_2 on cement hydration and its gel property. *Compos. Part B Eng.* **2013**, *45*, 440–448. [CrossRef]